Journal of Alloys and Compounds 517 (2012) 192–197

Contents lists available at SciVerse ScienceDirect

Journal of Alloys and Compounds

journal homepage: www.elsevier.com/locate/jallcom

Heterogeneous flammulina velutipes-like CdTe/TiO_2 nanorod array: A promising composite nanostructure for solar cell application

Bingwei Luo, Yuan Deng*, Yao Wang, Zhiwei Zhang, Ming Tan

Beijing Key Laboratory of Special Functional Materials and Film, School of Chemistry and Environment, Beihang University, Beijing 100191, China

ARTICLE INFO

Article history:
Received 26 September 2011
Received in revised form
19 December 2011
Accepted 19 December 2011
Available online 27 December 2011

Keywords:
Nanostructured materials
Nanofabrications
Photoconductivity and photovoltaics
Light absorption and reflection

ABSTRACT

Core–shell heterogeneous CdTe/TiO_2 nanorod arrays have been prepared by a two-step synthesis route through combined hydrothermal growth and magnetron sputtering. The composition and microstructure of the arrays were investigated by powder X-ray diffraction (XRD), scanning electron microscopy (SEM) and high-resolution transmission electron microscopy (HRTEM), which show that CdTe nanograins coated on the surface of the single-crystalline TiO_2 nanorod arrays to form a type-II heterostructure. Compared with TiO_2 nanorod arrays, the spectrum absorption region of CdTe/TiO_2 core–shell nanostructure is broadened from ultraviolet light to visible light. The photoelectrodes of CdTe/TiO_2 nanorod arrays show better photoelectric properties than those of bare TiO_2 nanorod arrays. The output power of CdTe/TiO_2 nanorod arrays is 25 times higher than that of a bare TiO_2 nanorod array. These results indicate that the photoelectrode of CdTe/TiO_2 nanorod array has a promising application in solar cell.

© 2011 Elsevier B.V. All rights reserved.

1. Introduction

TiO_2 is an important wide gap semiconductor with many applications such as photocatalysis, pollutant degradation and photovoltaic cells [1–4]. Recently, the one-dimensional TiO_2 nanostructures aimed at solar cells applications have attracted vast attention for their stable properties, efficient charge separation and transport properties [5–7]. However, these wide bandgap materials alone cannot absorb the sun light efficiently restricted by their narrow light absorption range [8]. Core–shell structure is always used to tune the basic optical properties of the core material such as Lin et al. synthesized ZnSe/ZnS of type-I core/shell structure, which remarkably improves the photoluminescence [9]. Meanwhile, type-II core–shell structure has both the valence and conduction bands in the core lower (or higher) than in the shell. As a result, one carrier is mostly confined to the core, while the other is mostly confined to the shell. Type-II structures can allow access to wavelengths that would otherwise not be available with a single material. In addition, the separation of charges in the lowest excited states of type-II nanocrystals should make these materials more suitable in photovoltaic or photoconduction applications [8,10].

Type-II core–shell structures with different band alignments, such as TiO_2/ZnO, ZnO/Er_2O_3, ZnO/ZnS, V_2O_5/ZnO, ZnSe/CdS or ZnO/CdTe, have been reported [11–16]. Those core–shell structures show adding light emission or enhanced efficiency of solar cells. Kang et al. fabricated an all-inorganic ZnO/ZnSe nanowires type-II p–n junction array which exhibits a threshold of 1.6 eV, corresponding to an efficiency of 29% under one-sun [17]. A cadmium telluride solar cell uses a cadmium telluride (CdTe) thin film, a semiconductor layer to absorb and convert sunlight into electricity. CdTe is a near perfect material for PV application with a direct band gap of 1.5 eV that is closely matched to the terrestrial solar spectrum and a high optical absorption coefficient where less than 1 μm thickness is adequate to absorb the incident light [18,19]. Thus, it is interesting that incorporating CdTe onto one-dimensional TiO_2 nanorods to form type-II band alignment, which may enhance the photoelectric current of the TiO_2. Here, we report a flammulina velutipes-like CdTe/TiO_2 core–shell heterogeneous nanostructure synthesized by a two-step route combined hydrothermal growth and magnetron sputtering. The coating of CdTe grains on the surface of TiO_2 nanorod arrays broadens the spectra absorption range and increases the photo induced current significantly, which suggests it a promising material to absorb and convert sunlight into electricity for solar cell application.

2. Experimental procedures

The two-step process to prepare CdTe/TiO_2 core–shell structure is described as follows: first, TiO_2 nanorod arrays were prepared on FTO substrate (F:SnO_2, 14 Ω/sq, Nippon Sheet Glass Group, Japan) using titanium butoxide as starting materials by a hydrothermal process at 150 °C for 20 h [5,20]. Then, the FTO substrate was

* Corresponding author. Fax: +86 10 82313482.
E-mail address: dengyuan@buaa.edu.cn (Y. Deng).

0925-8388/$ – see front matter © 2011 Elsevier B.V. All rights reserved.
doi:10.1016/j.jallcom.2011.12.090

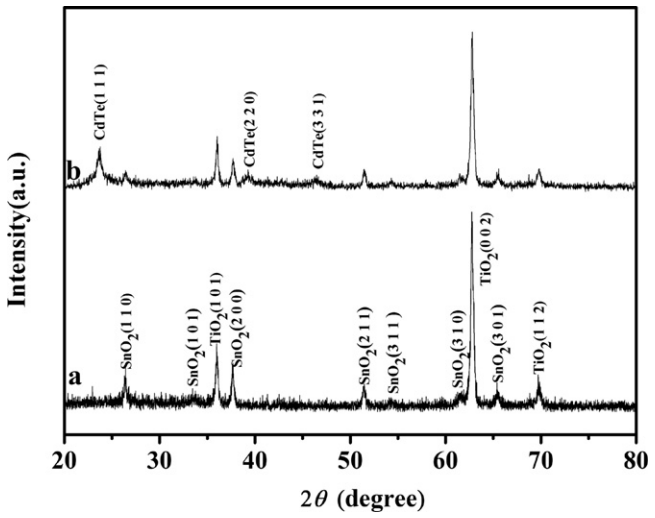

Fig. 1. XRD patterns of (a) TiO_2/FTO and (b) CdTe/TiO_2/FTO.

taken out, rinsed extensively with deionized water, and was dried in ambient air. Next, CdTe was deposited onto the surfaces of TiO_2 nanorods using radio-frequency (RF) magnetron sputtering at room temperature. Commercial hot-pressed CdTe target (99.9% in purity) with 60 mm diameter was used and the working pressure was controlled at 1.2 Pa using Ar carrier gas, and the sputtering power was 50 W.

The phase was identified with X-ray diffraction in the 2θ range from 10° to 100° with Cu Kα radiation (Rigaku D/MAX-2200 diffractometer, Japan). The microstructure of the composites was observed with a scanning electron microscopy (SEM, Hitachi S-6300) and high resolution transmission electron microscope (HRTEM, JEOL JEM-2100F). The composition was analyzed by using X-ray energy dispersive analysis (EDX). Diffuse reflectance absorption spectra were recorded by a Cintra.10e spectroscopy with $BaSO_4$ as a reference. The photocurrent intensity versus measured potential (*I–V* curves) of the samples was measured using an electrochemical analyzer (CHI 600D Instruments, China). The as-prepared sample was used as the working electrode, a platinum wire is used as the counter electrode, and a saturated Ag/AgCl electrode was used as the reference electrode. 1 M Na_2S aqueous solution was used as the electrolyte. The working electrode was illuminated from the back side within an area about 0.2 cm^2 with a solar-simulated light source (AM 1.5 G filtered, 100 mW/cm^2, 69911, Oriel). Photoluminescence (PL) spectra were collected at room temperature by a LabRAM HR800 (HORIBA Jobin Yvon) confocal Raman Spectrometer, with an excited wavelength at 325 nm using He–Cd laser.

3. Results and discussion

Fig. 1 shows the XRD patterns of the TiO_2/FTO and CdTe/TiO_2/FTO. SnO_2 glass substrate is rutile structure (JCPDS no. 41-1445), and the TiO_2 nanorod array grown on FTO shows a tetragonal rutile structure (Fig. 1a). The enhanced (0 0 2) peak intensity indicates the TiO_2 nanorods grew preferentially along [0 0 1] direction. CdTe/TiO_2/FTO was formed by the controllable deposition of CdTe onto the surfaces of TiO_2 nanorods. The optimized conditions are that the working pressure is at 1.2 Pa using Ar carrier gas and the sputtering power is 50 W. Compared with XRD patterns of TiO_2/FTO, the additional peaks appearing in those of CdTe/TiO_2/FTO can be attributed to CdTe phase with a zinc blende structure (JCPDS no. 15-0770).

The morphologies and microstructures of TiO_2/FTO and CdTe/TiO_2/FTO are shown in Fig. 2. Highly ordered TiO_2 nanorods are hydrothermal grown perpendicularly on the FTO substrate to give nanorod arrays. The shape of the TiO_2 nanorods is spear-like with the length of about 2.5 μm. The diameters of TiO_2 nanorods are 200–250 nm at bottom and about 100 nm at top (shown in Fig. 2a and b). The SEM images of the CdTe/TiO_2/FTO are shown in Fig. 2c–e, indicating the formed CdTe/TiO_2/FTO nanorods are flammulina velutipes-like. The surface of TiO_2 nanorod arrays is covered by spherical CdTe grains at the top of TiO_2 nanorod (shown in Fig. 2c and d). Seen from Fig. 2e, the diameters of the CdTe/TiO_2 nanorods become uniform from bottom to top and increase to 250–300 nm. An EDX results of a single CdTe/TiO_2 nanorod indicate the presence of elements Cd, Te, Ti, and O, with Cd/Te atomic ratio about 1:1 (shown in Fig. 2f).

The microscopic structures of the core/shell CdTe/TiO_2 nanorods are further characterized by TEM. Fig. 2g shows a low-magnification TEM image of a core–shell CdTe/TiO_2 nanorod, which clearly shows CdTe grains coating on the surface of TiO_2 nanorod form a core–shell structure. Meanwhile, it can be seen that the CdTe shell with totally around 200 nm is mainly deposited on the top of TiO_2 nanorods, and then the whole surface of TiO_2 nanorod with different thickness CdTe can be functionalized in the process of charge separation. A high-resolution TEM image of the interface region between TiO_2 core and CdTe shell (marked by the rectangle in the inset of Fig. 2h) is shown in Fig. 2h, the crystal boundary is observed between two phases. The lattice spacing in the right part of the image is measured to be 0.32 nm, corresponding to the (1 1 0) plane of tetragonal rutile TiO_2. The measured lattice spacing in the left part is 0.23 nm, corresponding to the (2 2 0) plane of the cubic phase of CdTe. Due to large mismatch between the crystal lattices of CdTe and TiO_2, the strain is released by forming several unit cells disordered area at the interface.

Diffuse reflectance absorption spectrum of CdTe/TiO_2/FTO is shown in Fig. 3, and the spectra of TiO_2/FTO nanorod array and CdTe/FTO were measured for comparison. All the thickness of the samples was about 2 μm. The absorption intensity of TiO_2/FTO nanorod arrays is much higher than the other two in the ultraviolet light range, and quickly drops to the lowest in the visible light range. The absorption intensity of CdTe/FTO maintains stable from 300 nm to 350 nm in the ultraviolet light range, and quickly increases to the similar value maintaining from 360 nm to 800 nm. While the absorbance of the heterogeneous core–shell CdTe/TiO_2 nanostructure is increased to double the absorbance of CdTe, and spectrum absorption region extends to visible light region compared with TiO_2 nanorod arrays. Therefore, a great increase in absorbance and broadening of light spectrum absorption region is achieved in the CdTe/TiO_2 core–shell nanorod array, making a step towards the application in solar cells.

Fig. 4 shows the *I–V* curves of CdTe/FTO, TiO_2/FTO and CdTe/TiO_2/FTO. For the TiO_2/FTO, the short circuit photocurrent intensity and open circuit photovoltage versus Ag/AgCl are 0.387 mA/cm^2 and 0.727 V, respectively; while the values of CdTe/TiO_2/FTO are 13.485 mA/cm^2 and 0.519 V, respectively. The output power of CdTe/TiO_2/FTO is about 25 times larger than that of TiO_2/FTO. In addition, the short circuit photocurrent intensity and open circuit photovoltage versus Ag/AgCl of CdTe/FTO are quite small, about 0.0241 mA/cm^2 and 0.094 V. It is probably attributed to the low conductivity of CdTe/FTO that the photo induced current cannot be exported.

Fig. 5 depicts the PL spectra of CdTe/FTO, TiO_2/FTO and CdTe/TiO_2/FTO over a large energy range. For CdTe/FTO, the PL spectra exhibits two main types of emissions located at 542 nm (2.29 eV) and 724 nm (1.71 eV), which correspond to the defect and energy band, respectively; While the main type emission in PL spectra of TiO_2/FTO caused by the energy band is situated at 539 nm (2.30 eV). The emission peak in PL spectra of CdTe/TiO_2/FTO is much lower than other two thin films from 400 nm to 1000 nm. The strong suppression of the PL emission spectra of the CdTe/TiO_2/FTO thin film implies that charge separation occurred before the recombination

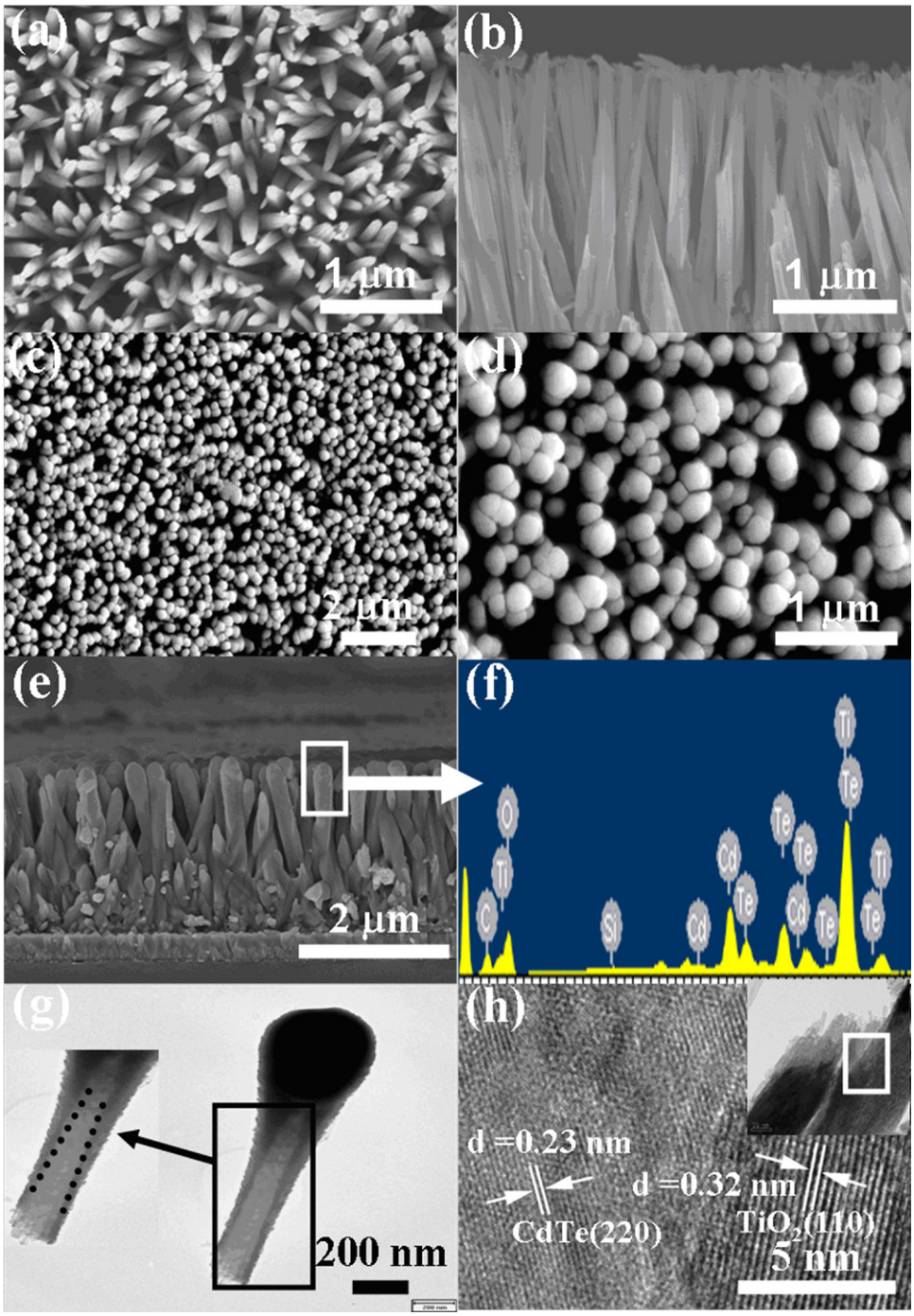

Fig. 2. SEM (a) surface and (b) cross-sectional images of TiO_2 nanorod array, (c–e) SEM surface and cross-sectional images of CdTe/TiO_2 core–shell nanorod array, (f) EDS collected from a single CdTe/TiO_2/FTO core–shell nanorod, (g) TEM top view image of CdTe/TiO_2 nanorods and (h) HRTEM image of CdTe/TiO_2 interface. The inset in (g) is enlarged image of core–shell nanowire tip and the inset in (h) is image of core–shell nanowire.

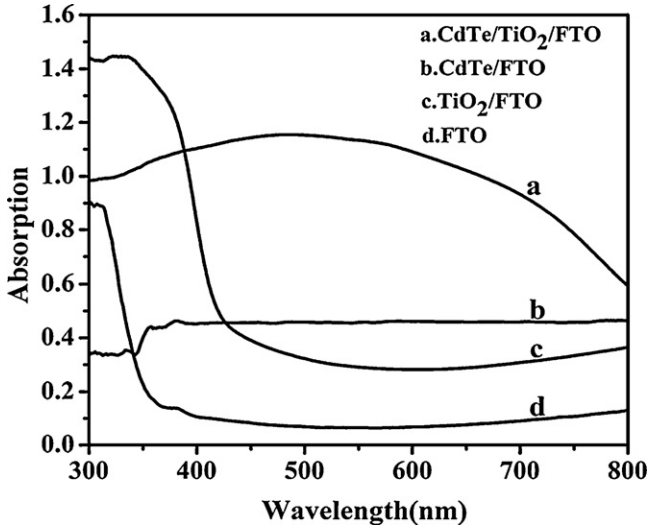

Fig. 3. Diffuse reflectance absorption spectra of (a) CdTe/TiO_2/FTO, (b) CdTe/FTO, (c) TiO_2/FTO, and (d) FTO.

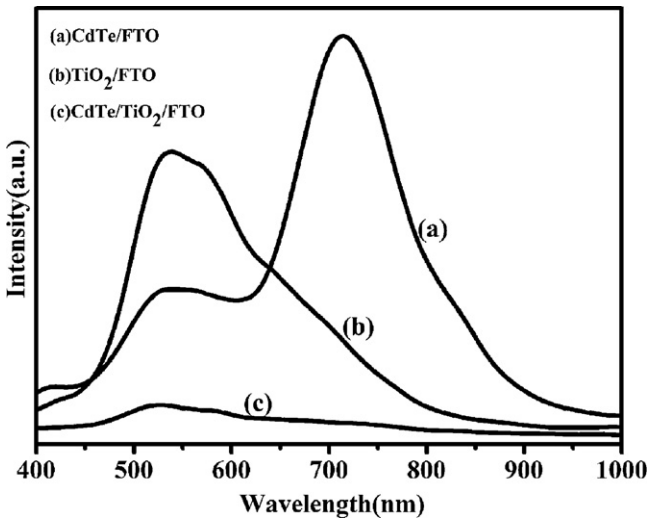

Fig. 5. Photoluminescence (PL) emission spectra of (a) CdTe/FTO, (b) TiO_2/FTO and (c) CdTe/TiO_2/FTO thin film. Strong suppression of the PL emission spectra of the CdTe/TiO_2/FTO implies that charge separation occurred before the recombination with CdTe.

with CdTe. It is concluded that the type-II core–shell heterostructure can separate electrons and holes to different components as opposed to charge collection to enhance the charge extraction efficiency.

The formation process of flammulina velutipes-like CdTe/TiO_2 nanorod arrays is illustrated in Fig. 6. Firstly, the TiO_2 nanorod arrays were prepared by the hydrothermal growth [20].

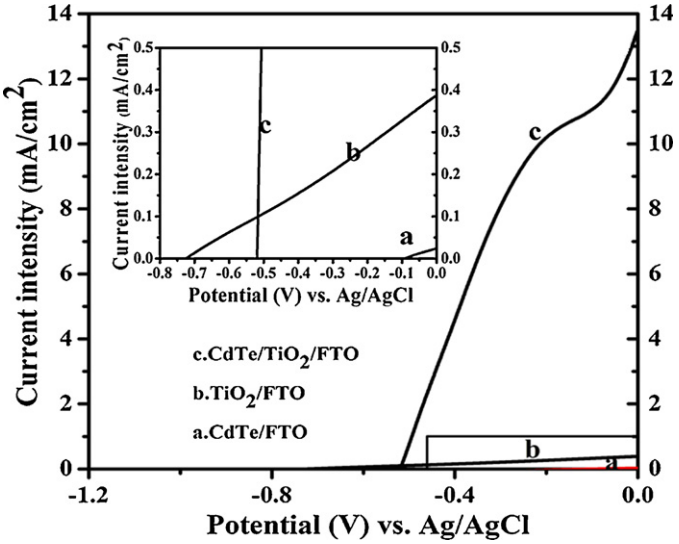

Fig. 4. *I–V* curves of (a) CdTe/FTO, (b) TiO_2/FTO, and (c) CdTe/TiO_2/FTO. All the samples were measured as photoelectrodes versus Ag/AgCl reference electrode under simulated sunlight with an illumination intensity of 100 mW/cm^2 in 1 M Na_2S aqueous solution.

Secondly, Cd and Te atoms were sputtered and deposited on the surface of TiO_2 nanorod arrays. Then, nucleation began and CdTe nanograins formed. The key for fabricating flammulina velutipes-like CdTe/TiO_2 nanorod array is to keep a proper crystal growth rate. When the crystal growth rate of CdTe atoms was higher than deposition rate (e.g., work pressure above 1.0 Pa and working power below 50 W), there were enough time for the nuclei to grow on the surface of TiO_2 nanorod array to form flammulina velutipes-like morphology. When the crystal growth rate of CdTe atoms was lower than deposition rate (e.g., work pressure below 0.5 Pa and working power above 80 W), the nuclei grew fast to the interspaces among of TiO_2 nanorod array resulting in the disorder morphology. Finally, CdTe/TiO_2 thin films with different structures were obtained on the FTO substrate.

The bandgap of CdTe shell is about 1.71 eV, which is smaller than that of TiO_2 core (about 2.30 eV), and the energies of both the conduction and valence bands of CdTe are higher than those of TiO_2, then CdTe/TiO_2 thin films form type-II core–shell structure (shown in Fig. 5). As a result, one carrier is mostly confined to the core, while the other is mostly confined to the shell. The following reasons are the main contributions to the enhancement of photoelectrical properties of the CdTe/TiO_2 nanorod arrays. Firstly, the staggered band alignment of the heterostructure leads to a smaller effective bandgap than each one of the constituted components, producing a red-shifted absorption [21,22]. Secondly, the type-II heterostructure, with shell thickness of about 200 nm, makes the holes and electrons are partially confined in the shell [21], and then, the energy gradient that exists at the interfaces can spatially separate electrons and holes to different components as opposed to charge collection to enhance the charge extraction efficiency [23]. Besides, the quantum confinement effect of the uniform morphology would effectively suppress the recombination of electrons and holes [24]. Thirdly, the flammulina velutipes-like morphology can separate the electrons and holes on the top and allow a fast and efficient transfer of the photo generated electrons from CdTe/TiO_2 nanorods to the conductive FTO substrate.

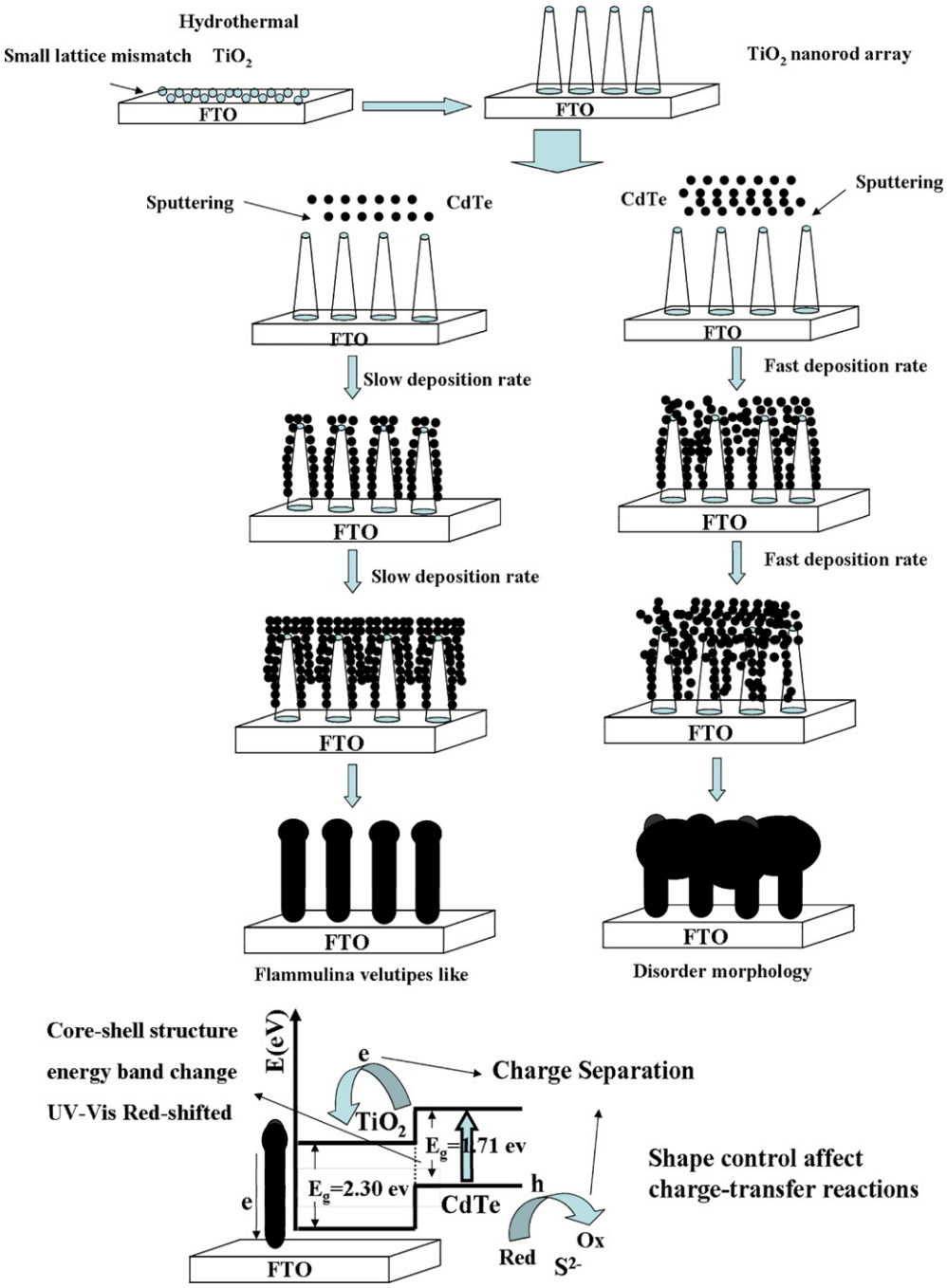

Fig. 6. Schematic diagram of growth mechanism of CdTe/TiO_2 nanorod arrays, energy band of CdTe/TiO_2 core–shell nanorod, and photo induced charge separation and transport in the heterostructure.

4. Conclusions

In summary, a heterogeneous flammulina velutipes-like CdTe/TiO_2 nanostructure has been prepared using a two-step synthesis route on the FTO substrate. The TiO_2 nanorods were coated with CdTe nanograins on the surface forming type-II core–shell heterostructure. This special nanostructure effectively broadens the absorption spectra, enhances the charge extraction efficiency by the electron and hole separation and provides a fast transfer channel for charge carriers. Therefore, the coating of CdTe grains on the surface of TiO_2 nanorod arrays broadens the spectra absorption range and increases the photo induced current significantly, which suggests it a promising material to absorb and convert sunlight into electricity for solar cell application.

Acknowledgments

This work was supported by the National Natural Science Foundation of China (Grant No. 51172008), the National High Technology Research and Development Program of China (Grant No. 2009AA03Z322). The authors are grateful to Dr. Hua Wang (Beihang University) for his kind help.

References

[1] Y. Zhang, X. Ma, P. Chen, D. Li, D. Yang, Appl. Phys. Lett. 94 (2009) 061115.
[2] H.J. Yan, H.X. Yang, J. Alloys Compd. 509 (2011) L26.
[3] P. Zhong, W.X. Que, J. Zhang, Q.Y. Jia, W.J. Wang, Y.L. Liao, X. Hu, J. Alloys Compd. 509 (2011) 7808.
[4] Y.L. Liao, W.X. Que, Z.H. Tang, W.J. Wang, W.H. Zhao, J. Alloys Compd. 509 (2011) 1054.
[5] H. Wang, Y.S. Bai, H. Zhang, Z.H. Zhang, J.H. Li, L. Guo, J. Phys. Chem. C 114 (2010) 16451.
[6] J. Shi, C.L. Sun, M.B. Starr, X.D. Wang, Nano Lett. 2 (2011) 624.
[7] J.Y. Liao, B.X. Lei, Y.F. Wang, J.M. Liu, C.Y. Su, D.B. Kuang, Chem.-Eur. J. 4 (2011) 1352.
[8] Y. Zhang, L. Wang, A. Mascarenhas, Nano Lett. 7 (2007) 1264.
[9] Z.H. Lin, M.Q. Wang, L.Z. Wei, X.H. Song, Y.H. Xue, X. Yao, J. Alloys Compd. 509 (2011) 8356.
[10] J. Schrier, D.O. Demchenko, L.W. Wang, Nano Lett. 7 (2007) 2377.
[11] C.W. Zou, X.D. Yan, J. Han, R.Q. Chen, W. Gao, Chem. Phys. Lett. 476 (2009) 84.
[12] S.Z. Li, C.L. Gan, H. Cai, C.L. Yuan, J. Guo, P.S. Lee, J. Ma, Appl. Phys. Lett. 90 (2007) 263106.
[13] K. Wang, J.J. Chen, Z.M. Zeng, J. Tarr, W.L. Zhou, Y. Zhang, Y.F. Yan, C.S. Jiang, J. Pern, A. Mascarenhas, Appl. Phys. Lett. 96 (2010) 123105.
[14] C.W. Zou, Y.F. Rao, A. Alyamani, W. Chu, M.J. Chen, D.A. Patterson, E.A.C. Emanuelsson, W. Gao, Langmuir 26 (2010) 11615.
[15] Z.J. Ning, H.N. Tian, C.Z. Yuan, Y. Fu, H.Y. Qin, L.C. Sun, H. Agren, Chem. Commun. 47 (2011) 1536.
[16] V. Consonni, G. Rey, J. Bonaimé, N. Karst, B. Doisneau, H. Roussel, S. Renet, D. Bellet, Appl. Phys. Lett. 98 (2011) 111906.
[17] Z.M. Wu, Y. Zhang, J.J. Zheng, X.G. Lin, X.H. Chen, B.W. Huang, H.Q. Wang, K. Huang, S.P. Li, J.Y. Kang, J. Mater. Chem. 21 (2011) 6020.
[18] Z.Z. Bai, J. Yang, D.L. Wang, Appl. Phys. Lett. 99 (2011) 143502.
[19] S. Shanmugan, D. Mutharasu, J. Alloys Compd. 509 (2011) 2143.
[20] B. Liu, E.S. Aydil, J. Am. Chem. Soc. 131 (2009) 3985.
[21] S.S. Lo, T. Mirkovic, C.H. Chuang, C. Burda, G.D. Scholes, Adv. Mater. 23 (2011) 180.
[22] P. Reiss, M. Protière, L. Li, Small 5 (2009) 154.
[23] M.A. Hossain, J.R. Jennings, Z.Y. Koh, Q. Wang, ACS Nano 5 (2011) 3172.
[24] N.J. Borys, M.J. Walter, J. Huang, D.V. Talapin, J.M. Lupton, Science 330 (2010) 1371.